

Periodicity of dynamical signatures of chaos in quantum kicked top

Sreeram P.G¹ and M.S. Santhanam¹

¹*Indian Institute of Science Education and Research, Pune 411008, India.*

(Dated: November 8, 2023)

A host of dynamical measures of quantum correlations – out-of-time ordered correlators, Loschmidt echo, generalized entanglement and observational entropy – are useful to infer the underlying classical chaotic dynamics in quantum regime. In this work, these measures are employed to analyse quantum kicked top with kick strength k . It is shown that, despite the differences in their definitions, these measures are periodic with k , and the periodicity depends on the number of spins represented by the kicked top. The periodic behaviour arises from the structure of the kicked top Floquet operator and spans the regime in which the corresponding classical dynamics is predominantly chaotic. This result can guide experiments towards the right choice of kick strengths to avoid repetitive dynamics.

I. INTRODUCTION

The manifestations of classical chaos in quantum systems is central to our evolving understanding of quantum chaotic systems. The statistical properties of spectra of quantum systems whose classical counterpart is chaotic are consistent with that of an appropriate ensemble of random matrix theory (RMT) [1, 2]. A good agreement between the statistics of the empirical and RMT spectrum is usually taken to imply the presence of quantum chaos. In contrast, the spectra of quantum systems whose classical limit displays regular dynamics are uncorrelated and display Poisson statistics [3]. In the last four decades, spectral statistics have been an essential tool to infer the nature of underlying classical dynamics – whether it is regular, chaotic or of mixed type. Recently, it was shown for a quantized triangle map that RMT-type spectral correlations can arise even if the underlying classical system is only ergodic and not chaotic [4].

Despite the success of spectral correlations, such as the level spacing distributions as a diagnostic tool for quantum chaos [5, 6], they can capture only limited information about dynamics, and it is not straightforward. For instance, mean level spacing can provide coarse information about typical timescales of dynamics, but using spectral gaps to infer about the time evolution of arbitrary initial states is usually not easy [7, 8]. Temporal evolution is important for the following reason. In classical systems, the nature of dynamics, whether it is chaotic or regular, can be inferred from the Lyapunov exponent, which is obtained from the time evolution of trajectories. To be on the same footing, it is desirable to characterise quantum systems using measures based on the time evolution of arbitrary initial states.

The Out-of-Time Ordered correlator (OTOC), Loschmidt echo (LE), generalized entanglement and observational entropy (OE) are among the measures that are currently being extensively studied in the context of few- and many-body quantum chaos [9–17]. Dynamical signatures of quantum chaos, such as out-of-time-ordered correlators, have emerged as an important proxy to infer the presence of exponential divergence of trajectories in

the classical limit. In particular, OTOCs can distinguish between ergodicity and true chaos in classical systems [4]. In contrast to other dynamical measures such as Loschmidt echo, an attractive feature of OTOC is that its growth rate within the Ehrenfest timescale is proportional to that of the classical Lyapunov exponent. Hence, the OTOC growth rate can be conveniently used as a “quantum analogue” of the classical Lyapunov exponent.

Loschmidt echo [13, 14] is closely related to the OTOC, which deals with the fidelity decay of a state subject to imperfect time reversal. Since exact time reversal is impossible in practice, any small error amplifies rapidly and reflects in the fidelity decay when the dynamics is chaotic. The other two dynamical measures we consider in this paper are generalized entanglement and observational entropy. Generalized entanglement was defined in quantum systems with no natural subsystem decomposition [18]. Effectively, generalized entanglement is a subsystem-independent generalization which coincides with traditional entanglement when natural subsystems are considered. It was shown that generalized entanglement captures signatures of chaos in a kicked top [19]. Observational entropy (OE) is the quantum analogue of the statistical entropy studied in [20]. Observational entropy was recently shown to characterise chaos in a quantum kicked top [16]. The motivation to investigate OE for signatures of chaos originates from the close connection between the coarse-grained classical entropy in Ref. [20] with the Kolmogorov-Sinai entropy rate.

To study these quantities, we employ the quantum kicked top (QKT) as our model of choice. It is a popular model of time-dependent quantum chaos [21–23]. It represents the dynamics of angular momentum vector on a sphere with free rotations about one of the axes, and periodic torsion (kick) applied about some other axes. If the strength of periodic kicks is large, the classical limit of kicked top is chaotic. Quantum kicked top is a simple, useful and yet non-trivial model that serves as a test bed for asking fundamental questions about chaos and thermalization [21, 24]. They were experimentally realised in laser-cooled atoms [23], superconducting systems [24],

and NMR platform [25]. The QKT model can be thought of as a collection of interacting spins in which every spin interacts with every other spin. Recently, it was shown that few-spin QKTs are analytically solvable [26, 27]. Interestingly, even when the kicked top is represented in terms of just four spins (a deep quantum limit), an exponential growth of OTOC is observed with potential for experimental measurements.

Recently, it was observed that the entanglement entropy and quantum discord, when applied to QKT, displayed periodicity with respect to the kick strength (chaos parameter) k , and also with respect to time in a limited sense. One consequence is that if we wish to avoid a periodic behaviour of these measures, then a constraint on the minimum number of spins comes into play. In this article, we probe if the dynamical characterisers of quantum chaos, such as OTOC, Loschmidt echo and two other entropy measures – generalized entanglement and observational entropy – also display periodic behaviour. The periodicities we report for these measures are different from those reported in Ref. [28] for entanglement and quantum discord. Though kicked top dynamics is obtained by the stroboscopic evolution under repeated unitary operations, periodicity is usually not seen in the evolving observables. Such periodicities are not known for quantum kicked rotor. Hence, the existence of periodicities is both a curiosity and also has experimental consequences as we describe in the rest of the work.

The rest of this article is organized as follows. In the next section, we provide an overview of quantum kicked top. Sections III to VI the periodicity of dynamical signatures of chaos, starting with that of OTOC. Finally, section VII concludes by highlighting the utility of these results.

II. QUANTUM KICKED TOP

Quantum kicked top (QKT) is one of the well-studied models of quantum chaos in time-dependent systems. The Hamiltonian of the QKT is

$$H(t) = \alpha J_y + \frac{k}{2j} J_z^2 \sum_{m=-\infty}^{\infty} \delta(t - m), \quad (1)$$

in which both the Planck's constant and kick period are set to unity. The first term represents precession about the y -axis with angular frequency α , while the second term describes an instantaneous rotation proportional to J_z (torsion) about z -axis at periodic time intervals (set to unity). The latter is referred to as the “kick” term, indicating its impulsive nature. The parameter k is the strength of the periodic kick. Due to the periodic kicks, quantum dynamics can be conveniently studied through the period-1 Floquet operator given as

$$U(k) = \exp\left(-i\frac{k}{2j}J_z^2\right)\exp(-i\alpha J_y). \quad (2)$$

The action of this unitary operator on a quantum state $|\psi(0)\rangle$ describes its evolution such that the evolved wave function after m time steps is

$$|\psi(m)\rangle = U^m(k) |\psi(0)\rangle. \quad (3)$$

The evolution of the angular momentum operator can be seen in the Heisenberg picture as

$$J'_i = U^\dagger(k) J_i U(k), \quad i = x, y, z. \quad (4)$$

Since $U(k)$ commutes with J^2 , the angular momentum is conserved, and the dynamics of $\{J_x, J_y, J_z\}$ is confined to the surface of a 2-dimensional sphere. To study the classical limit of top, spin-coherent states are used, aligning \bar{j} with minimum uncertainty along a direction parametrized by two angles, (θ, ϕ) . The classical limit can be obtained by taking $j \rightarrow \infty$. Defining $X = \left\langle \frac{J_x}{j} \right\rangle$, $Y = \left\langle \frac{J_y}{j} \right\rangle$, and $Z = \left\langle \frac{J_z}{j} \right\rangle$, where the expectation values are with respect to spin-coherent states, we get a classical map (Eq. 43 in the supplementary information), which after setting $\alpha = \pi/2$ simplifies to the form [21]

$$\begin{aligned} X' &= Z \cos(kX) + Y \sin(kX), \\ Y' &= -Z \sin(kX) + Y \cos(kX), \\ Z' &= -X. \end{aligned} \quad (5)$$

It must be noted that the results obtained in this work span over parameter ranges of $k \gg 1$ for which the classical dynamics is mostly chaotic. This implies that our periodicity results are quantum in origin and arise from the structure of the Floquet operator in Eq. 2.

III. OTOC FOR KICKED TOP

Out-of-time-ordered correlators (OTOC) have emerged as a measure of quantum chaos since they could be thought of as “quantum Lyapunov exponent” analogous to the classical Lyapunov exponent [9–11]. For chaotic systems, they display a quantum analogue of the butterfly effect, a classic feature of chaos. Consider a system described by a quantum state $|\psi\rangle$, evolving under a Hamiltonian H . OTOC is defined with respect to two operators, denoted by V and W , which can be unitary or Hermitian. These operators can be considered to be locally acting on distinct subspaces in the Hilbert space, so they are initially commuting. At time $t = 0$, we have $[V, W] = 0$. Now, one of them, say W is evolved in the Heisenberg picture under the global Hamiltonian: $W(t) = e^{-iHt} W e^{iHt}$, and as a result, its support grows in the Hilbert space. This can be seen as a perturbation W preventing the cancellation of forward and backward evolution, reminding one of the classical butterfly effect. For $t > 0$, the operator $W(t)$ no longer commutes with V . The rate of growth of $\langle [V, W(t)]^2 \rangle$ captures the growth of $W(t)$, or the scrambling of information in

the Hilbert space. As the classical limit is approached, this growth rate is exponential for classically chaotic systems, with the exponent reflecting the classical Lyapunov exponent. The OTOC is formally defined as

$$C_{V,W}(t) = -\frac{1}{2} \text{Tr}(|\psi\rangle\langle\psi| [W(t), V]^2), \quad (6)$$

where the expectation is taken with respect to the system state $|\psi\rangle$. This work deals with infinite temperature OTOC, defined as

$$C_\infty(t) = C(t) = -\frac{1}{2} \text{Tr}\left(\frac{I}{d}[W(t), V]^2\right). \quad (7)$$

Here the expectation value is taken in the thermal state $\rho_\beta = e^{-\beta H}/\text{Tr}(e^{-\beta H})$, where $\beta = 1/K_B T \rightarrow 0$. To study the OTOC properties of the kicked top operator in Eq. 2, we evolve an arbitrary operator $W = W(0)$ for m iterations using

$$W(m; k) = U^m(k) W U^{\dagger m}(k), \quad m = 1, 2, 3, \dots, \quad (8)$$

where k is the strength of the kick applied to the top. In terms of Eq. 7, our object of interest is the time-evolving OTOC given by

$$C(m; k) = -\frac{1}{2} \text{Tr}\left(\frac{I}{2j+1} [W(m; k), W]^2\right). \quad (9)$$

A. Periodicity of OTOC with kick strength k

The central result we shall discuss below is that, for the kicked top system, measures such as OTOC, Loschmidt echo, generalized entanglement and observational entropy display periodic behaviour as a function of kick strength k . Let us begin by analyzing the occurrence of periodicities in OTOC under a change of parameter, i.e., we are seeking invariance of OTOC under the transformation $k \rightarrow k + \kappa_j$ for some periodicity κ_j . The operator in Eq. 2 under this transformation will become

$$\begin{aligned} U(k + \kappa_j) &= \exp\left(-i\frac{k + \kappa_j}{2j} J_z^2\right) \exp(-i\alpha J_y), \\ &= \exp\left(-i\frac{\kappa_j}{2j} J_z^2\right) U(k). \end{aligned} \quad (10)$$

If OTOC must remain invariant under $k \rightarrow k + \kappa_j$, then we will require that

$$\exp\left(-i\frac{\kappa_j}{2j} J_z^2\right) = z \mathcal{I}_d, \quad (11)$$

where z is some complex number with $|z| = 1$, and \mathcal{I}_d is the identity operator. This condition can be satisfied for positive integer values of j if $\kappa_j = 4p\pi j$ so that

$$\exp(-i2p\pi j^2) = \mathcal{I}_d, \quad p = 1, 2, 3, \dots \quad (12)$$

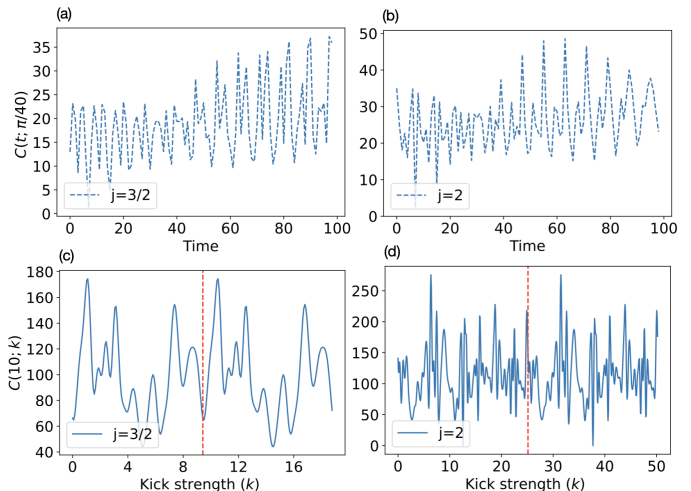


FIG. 1: The top panel shows time evolution of $C(m; k)$ with $k = \pi/40$ for (a) $j = 3/2$ and (b) $j = 2$. They do not show any periodicity in time. The bottom panel shows the k -periodicity in $C(m = 10; k)$ generated by a random Hermitian operator W at $\alpha = \pi/4$ for (c) $j = 3/2$, the red (dashed) line at $\kappa_j = 2\pi j = 3\pi \approx 9.42$, marks one period, and (d) $j = 2$, (dashed) line at $\kappa_j = 4\pi j = 8\pi \approx 25.13$, marks one period.

The condition in Eq. 11 can also be satisfied for positive half-integer values of j if $\kappa_j = 2p\pi j$ so that

$$\exp(-ip\pi j^2) = \frac{1}{\sqrt{2}}(1 - i)\mathcal{I}_d. \quad (13)$$

To realize periodicity, let us evolve the operator W in OTOC as follows:

$$\begin{aligned} W(m; k + \kappa_j) &= U^m(k + \kappa_j) W U^{\dagger m}(k + \kappa_j) \\ &= \left[\exp\left(-i\frac{\kappa_j}{2j} J_z^2\right) U(k) \right]^m W \left[U^\dagger \exp\left(i\frac{\kappa_j}{2j} J_z^2\right) \right]^m \\ &= U^m(k) W U^{\dagger m}(k) = W(m; k) \end{aligned} \quad (14)$$

The last equality is obtained by using the condition in Eq. 11. Thus, using Eqs. 12-13, the central result can be stated as

$$\begin{aligned} C(m; k) &= C(m; k + \kappa_j), \quad \kappa_j = 4p\pi j, \quad j \in \mathbb{Z}^+ \\ &= C(m; k + \kappa_j), \quad \kappa_j = 2p\pi j, \quad j \in \mathbb{Z}^+ - \frac{1}{2}, \end{aligned} \quad (15)$$

where \mathbb{Z}^+ denotes the set of positive integers and $\mathbb{Z}^+ - \frac{1}{2}$ is the set of positive half-integers. At any fixed time step m , we can recognise two distinct periodicities depending on j . Note that this argument does not involve J_y operator in Eq. 2 and κ_j is valid for any value of α .

To demonstrate this periodicity through simulations, we have chosen W to be a random matrix drawn from the Gaussian orthogonal ensemble (GOE) of random matrix

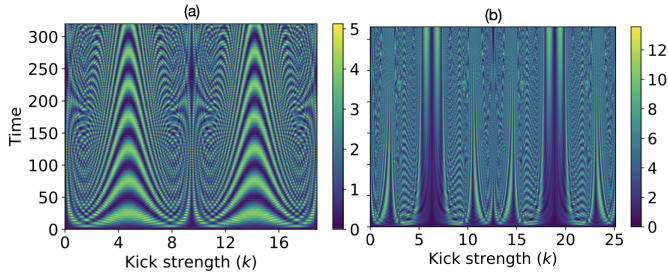


FIG. 2: Image plot of $C(m; k)$ with $\alpha = \pi/4$. (a) For $j = 3/2$, periodicity of $\kappa_j = 2\pi j$ occurs for all m . (b) For $j = 2$, periodicity of $\kappa_j = 4\pi j$ occurs for all m .

theory. With this choice, the temporal growth of OTOC $C(m; k)$ at a fixed value of k generally does not show any periodicity (see Sec. IIIB for an exception), as seen in Fig. 1(a,b) for $C(m; k)$ at $k = \pi/40$. In these cases, periodicity in time is not observed, though only a short time snapshot is shown for clarity. It turns out that the combination $k = \pi/40$ and $j = 1$ is an exceptional case which shows periodicity in time for rational values of k as we will discuss later.

However, as seen in Fig. 1(c,d), $C(10; k)$ as a function of k displays a periodicity of $4\pi j$ as anticipated by Eq. 15 with $p = 2$. The seemingly random pattern of the OTOC $C(m; k)$ in Fig. 1(c,d) (as a function of k) depends on the choice of the operator W . Each different choice of W gives rise to a different random-looking but periodic pattern. Irrespective of the choice of W , Eq. 15 guarantees that OTOC will always display periodicity with k as obtained in Eq. 15. Although we choose $m = 10$ in Fig. 1(c,d) for illustration, the periodicity in k is independent of the time. To show this, we plot an OTOC for an extended time in Fig. 2. The same periodicities mentioned above can be identified from the figure.

We discuss two special cases; periodicities that are consistent with Eq. 15 and yet $\kappa_j < 2\pi j$ or $\kappa_j < 4\pi j$. For example, at integer j and $\alpha = \pi/2$, the κ_j is $2\pi j$, at $m = \text{odd integer} \times 4$, and πj , at $m = \text{even integer} \times 4$. For other values of m , the period is $4\pi j$. Lower κ_j at multiples of four can be seen from the following equations.

$$\left[\exp\left(-i\frac{k+2\pi j}{2j}J_z^2\right) \exp(-i\alpha J_y) \right]^{(2p+1)\times 4} = U^{(2p+1)\times 4} \quad (16)$$

$$\left[\exp\left(-i\frac{k+\pi j}{2j}J_z^2\right) \exp(-i\alpha J_y) \right]^{2p\times 4} = U^{2p\times 4} \quad (17)$$

where p is an integer. OTOC generated by a random Hermitian operator A of the form $-\frac{1}{2} \text{Tr}\left(\frac{J}{d}[A(m), A(0)]^2\right)$, always follow the above periodicity.

Finally, we note that periodicities smaller than $4\pi j$ for $j \in \mathbb{Z}^+$ are observed in some cases where $W(0)$ and $W(t)$ are the same operators at different times. One such special case is illustrated in Fig. 3 for the OTOC given by $-\frac{1}{2} \text{Tr}\left(\frac{J}{d}[J_z(m), J_z(0)]^2\right)$. Further, it is seen that if

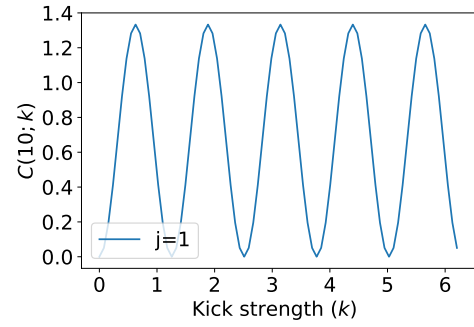


FIG. 3: OTOC $C(10; k) = -\frac{1}{2} \text{Tr}\left(\frac{J}{d}[J_z(10), J_z(0)]^2\right)$ as a function of k for $j = 1$, $\alpha = \pi/2$. Note that periodicity is smaller than $2\pi j$.

$\alpha \neq \pi/2$, a periodicity of $\kappa_j = 4\pi j$ is observed for $j \in \mathbb{Z}^+$ regardless of m and the operators constituting the OTOC. For $j \in \mathbb{Z}^+ - \frac{1}{2}$, periodicities smaller than $2\pi j$ is not observed regardless of the choice of operators, m and α .

B. Special cases of time periodicity

In this subsection, we study the periodicity in $C(m; k)$ with $j = 1$ and $\alpha = n\pi$ ($n \in \mathbb{Z}$). The unitary operator $U(k)$ with $n = 1$ and $\alpha = \pi$ has a rather simple form:

$$U(k) = \begin{pmatrix} 0 & 0 & e^{-ik/2} \\ 0 & -1 & 0 \\ e^{ik/2} & 0 & 0 \end{pmatrix}. \quad (18)$$

The operator for after m iterations yields

$$U^m(k) = \begin{pmatrix} \alpha_m & 0 & \beta_m \\ 0 & (-1)^m & 0 \\ \beta_m & 0 & \alpha_m \end{pmatrix}, \quad (19)$$

where $\alpha_m = \frac{1}{2} \left((e^{-\frac{ik}{2}})^m + (-e^{-\frac{ik}{2}})^m \right)$ and $\beta_m = \frac{1}{2} \left((e^{-\frac{ik}{2}})^m - (-e^{-\frac{ik}{2}})^m \right)$. The structure of these matrix elements is such that for any integral m , either $\alpha_m = 0$ or $\beta_m = 0$. Therefore, we always get $U^m(k)$ to be a diagonal or an anti-diagonal matrix with two corner matrix elements being $u_{1,2j+1} = u_{2j+1,1} \neq 0$.

This special structure of the unitary leads to a time periodicity of OTOC. When $k = r\pi/s$, ($r, s \in \mathbb{Z}$), we find a time period of $4s$ for odd r , and $2s$ for even r values. This is easily seen from the functional form of α_m and β_m . For instance, when m is even and $k = r\pi/s$, we have that $\alpha_m = \cos(km/2) = \cos(r\pi m/2s)$. Now,

$$\alpha_{m+4s} = \cos\left(\frac{r\pi(m+4s)}{2s}\right) = \cos\left(\frac{km}{2} + 2r\pi\right). \quad (20)$$

Since r is an integer, $\cos\left(\frac{km}{2} + 2r\pi\right) = \cos\left(\frac{km}{2}\right)$, and therefore $\alpha_m = \alpha_{m+4s}$. When r is an even integer, one

can easily verify that $\alpha_{m+2s} = \alpha_m$. The same arguments follow when m is an odd integer and for β_m . We have numerically verified this periodicity by choosing random operators for OTOCs.

IV. PERIODICITY IN LOSCHMIDT ECHO

Loschmidt echo (LE) is another well-known dynamical measure of quantum chaos [13, 15]. It is closely related to OTOC through a formal connection that relates OTOC to the thermal average of Loschmidt echo [29]. Consider an initial state $|\psi_0\rangle$, evolving under the unitary $\exp(-iHt)$, such that $|\psi(t)\rangle = \exp(-iHt)|\psi_0\rangle$, at time t . Now, to recover the initial state, in principle, we can get back to $|\psi_0\rangle$ by evolving with a Hamiltonian $-H$, for a time t . However, such a perfect time reversal is realistically impossible in a laboratory because of environmental influence and other experimental errors. Hence, a slightly different unitary operator $\exp(iH't)$, can be implemented where H' is slightly perturbed from H . Then Loschmidt echo being the overlap between the initial state $|\psi_0\rangle$ and the recovered state $|\psi'_0\rangle$ is given by

$$\mathcal{F}(t; H, H', |\psi_0\rangle) = |\langle \psi_0 | \exp(iH't) \exp(-iHt) | \psi_0 \rangle|^2. \quad (21)$$

Evidently, Loschmidt echo is a function of the initial state $|\psi_0\rangle$, the nature unitary dynamics, the strength and the nature of perturbation. For classically chaotic systems, LE shows rapid decay as a function of time and the decay rate depends on the Lyapunov exponent in certain regimes. For smaller perturbations, however, the decay is Gaussian.

The state dependence of LE can be removed by averaging over all the pure states under the Haar measure. In the kicked top Hamiltonian, forward time evolution depends on kick strength k , while the time-reversed dynamics depends on k' . With time m taking integer values, the averaged LE is given by

$$F(m; k, k') = \int d|\psi_0\rangle \mathcal{F}(m; k, k', |\psi_0\rangle), \quad (22)$$

yielding a state-independent function [30, 31]

$$F(m; k, k') = \frac{1}{d(d+1)} \left[d + |\text{Tr}(U^{-m}(k')U^m(k))|^2 \right]. \quad (23)$$

The connection between OTOC and LE can be argued out as follows. The OTOC for kicked top in Eq. 9 was defined in terms of operator $W(0)$ and its time-evolved version $W(m) = e^{-iHm}W e^{iHm}$ with $m \neq 0$. Then, $W(m)$ can be seen as a unitary perturbation of $W(0)$ preventing the cancellation of forward and backward evolution. This eventually results in a nontrivial growth of the squared commutator $[W(m), W]^2$ in the chaotic case. Thus, viewed this way, OTOC contains some elements of inequivalent forward and backward evolution captured by Loschmidt echo.

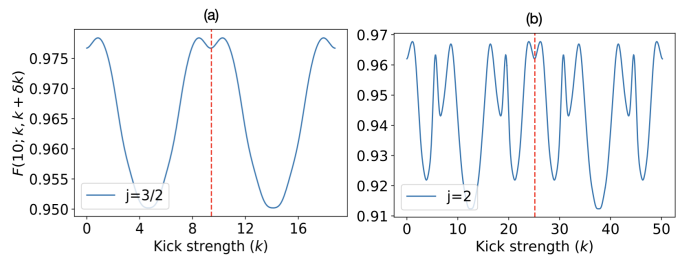


FIG. 4: (a) Periodicity of the Loschmidt echo for $j = 3/2$, $\alpha = \pi/4$, $m = 10$ and $k' = k + 0.1$. The red vertical line is at $\kappa_{3/2} = 2\pi j = 3\pi \approx 9.42$, marking one period. (b) Periodicity of the Loschmidt echo for $j = 2$, $\alpha = \pi/4$, $m = 10$ and $k' = k + 0.1$. The red vertical line is at $\kappa_2 = 4\pi j = 8\pi \approx 25.13$, marking one period.

To explore the periodicity of LE in k , we assume that $k' = k + \delta k$ in Eq. 23 and demand that

$$F(m; k, k + \delta k) = F(m; k + \kappa_j, k + \kappa_j + \delta k) \quad (24)$$

should hold for all fixed values of integer times m . It is straightforward to show that Eq. 24 can be satisfied by periodicity κ_j identical to that for OTOC :

$$\begin{aligned} \kappa_j &= 4p\pi j, \quad j \in \mathbb{Z}^+ \\ &= 2p\pi j, \quad j \in \mathbb{Z}^+ - \frac{1}{2}. \end{aligned} \quad (25)$$

independent of other parameters. Figure 4 displays the numerically simulated echo for kicked top system, confirming the periodicities predicted by Eq. 25. We would like to emphasise that the period κ_j is also independent of the amount of perturbation, δk .

Like OTOC, Loschmidt echo also displays κ_j smaller than allowed by Eq. 25 but without violating the general rules in Eq. 25. For instance, when $\alpha = \pi/2$, Eq. 23 yields a period of $2\pi j$ when $j \in \mathbb{Z}^+ - \frac{1}{2}$, and πj , when $j \in \mathbb{Z}^+$. These can be verified using the analytical expressions in Ref. [27]. For $j = 3/2$ and $\alpha = \pi/2$, Eq. 23 gives

$$F(m; k, k') = |\alpha_m \tilde{\alpha}_m^* + \beta_m \tilde{\beta}_m^* + \beta_m^* \tilde{\beta}_m + \alpha_m^* \tilde{\alpha}_m|^2, \quad (26)$$

$$\begin{aligned} \alpha_m &= T_m(\chi) + \frac{i}{2} U_{m-1}(\chi) \cos(k/3) \\ \beta_m &= \frac{\sqrt{3}}{2} U_{m-1}(\chi) \exp(ik/3), \end{aligned} \quad (27)$$

where $\chi = \sin(k/3)/2$, T_m and U_m are Chebychev polynomials of the first and second kind, respectively. They are defined as

$$T_m(\cos \theta) = \cos(m\theta), \quad U_m(\cos \theta) = \frac{\sin((m+1)\theta)}{\sin \theta}.$$

In Eq. 27, $\chi = \cos \theta = \sin(k/3)/2$. Substituting $k \rightarrow k + 2\pi j = k + 3\pi$, and $k' \rightarrow k' + 3\pi$, we get

$$\alpha_m = \begin{cases} \alpha_m^*, & m \text{ even,} \\ -\alpha_m^*, & m \text{ odd,} \end{cases} \quad (28)$$

$$\beta_m = \begin{cases} \beta_m, & m \text{ even,} \\ -\beta_m, & m \text{ odd.} \end{cases} \quad (29)$$

Substituting these back in Eq. 26, it is easy to see that $F(m; k, k')$ remains invariant for all m . Therefore, $F(m; k, k') = F(m; k + 2\pi j, k' + 2\pi j)$ for all $k, k' \in (0, 2\pi j)$. Any smaller translation of k than by $2\pi j$ will not have this property.

Similarly, one can verify the periodicity for $j = 2$. Eq. 23 leads to [27]

$$F(m; k, k') = \frac{1}{30} \left(5 + |1 + e^{im\delta k/4}(\alpha_m \tilde{\alpha}_m^* + \beta_m \tilde{\beta}_m^* + \beta_m^* \tilde{\beta}_m + \alpha_m^* \tilde{\alpha}_m + 2e^{3im\delta k/4} \cos^2(m\pi/2) + \sin^2(m\pi/2) \cos^2(3\delta k/8)|^2 \right), \quad (30)$$

where δk refers to the strength of the perturbation, which hampers the time reversal [27]. For $j = 2$, the terms α_m and β_m take the form

$$\begin{aligned} \alpha_m &= T_m(\chi) + \frac{i}{2} U_{m-1}(\chi) \cos(k/2) \\ \beta_m &= \frac{\sqrt{3}}{2} U_{m-1}(\chi) \exp(ik/2), \end{aligned} \quad (31)$$

where $\chi = \sin(k/2)/2$. Taking $k \rightarrow k + \pi j = k + 2\pi$, and $k' \rightarrow k' + 2\pi$, we get the same conditions as in Eq. 28 and 29. Under those transformations, the function $(\alpha_m \tilde{\alpha}_m^* + \beta_m \tilde{\beta}_m^* + \beta_m^* \tilde{\beta}_m + \alpha_m^* \tilde{\alpha}_m)$ remains invariant, and hence the function $F(k, k', m)$.

In addition to the periodicity in kick strength, we point out the existence of a reflection symmetry about $\kappa_j/2$ for Loschmidt echo, which can be observed in Fig. 4. For $j \in \mathbb{Z}^+$, and a set of the chaos parameters $k_1, k'_1 \in (0, 2\pi j)$, this symmetry arises due to the existence of simple relationships of the form

$$F(m; k_1, k'_1) = F(m; 4\pi j - k_1, 4\pi j - k'_1). \quad (32)$$

Similarly, for half-integer j , a reflection symmetry about $k = \pi j$ exists. This symmetry is independent of α and δk . This reflection symmetry is similar to that reported for several quantum correlations such as entanglement and quantum discord [28].

V. PERIODICITY IN GENERALIZED ENTANGLEMENT

Generalized entanglement (GE) was introduced as a subsystem-independent generalization of entanglement [32]. The conventional entanglement is applicable when the system has a natural subsystem decomposition and is quantified using the fact that a pure state in the composite system looks mixed to subsystem observers. The von Neumann entanglement entropy measures the subsystem purity to quantify the entanglement correlation between subsystems. Generalizing this, one can define purity with

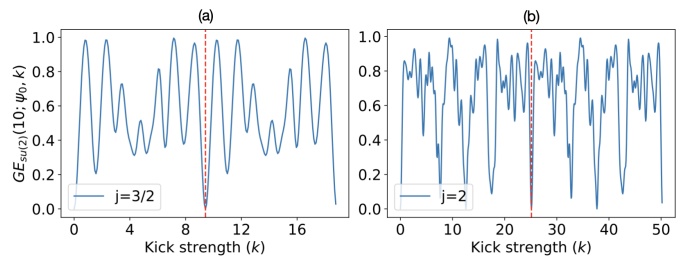


FIG. 5: Periodicity of the generalized entanglement with $\alpha = \pi/4$ for (a) $j = 3/2$ and $m = 10$, the red (dashed) line marks the expected periodicity based on Eq. 37 drawn at $\kappa_{3/2} = 2\pi j = 3\pi \approx 9.42$. (b) for $j = 2$ and $m = 10$, the red (dashed) line is drawn at $\kappa_2 = 4\pi j = 8\pi \approx 25.13$.

respect to a set of *distinguished observables* without referring to subsystems. This is useful when the system does not have a natural tensor product structure. The set of distinguished observables constitutes the limited means of measuring the system, analogous to a subsystem observer, who can only measure local observables. If the system has a natural subsystem decomposition, then one can get back standard entanglement by choosing the set of all uni-local observables corresponding to a subsystem [18].

Let $|\psi_0\rangle$ denote a pure state in Hilbert space \mathcal{H} . Using a chosen set of observables $\Omega = \{\mathcal{A}_l\}_{l=1}^L$, generalized purity by measurement can be defined as

$$P_\Omega(\psi_0) = K \sum_l |\langle \psi_0 | \mathcal{A}_l | \psi_0 \rangle|^2, \quad (33)$$

where K normalizes maximum purity to one. Then, with respect to the set Ω generalized entanglement is defined as $\text{GE}_\Omega = 1 - P_\Omega$. Physically, GE quantifies the extent of a state with respect to a set of operators [19]. The extent of states in different directions can distinguish a regular motion from a chaotic one [33, 34].

For the kicked top, Ω is chosen to be J_x, J_y, J_z , forming an irreducible representation of $su(2)$ Lie algebra. On projecting to this space of operators, the reduced states form a unit sphere, with the surface points comprising of generalized coherent states. Such extremal states are said to be *generalized unentangled* with respect to Ω . States lying inside the unit ball are mixed, implying they are *generalized entangled*. GE is established as a signature of chaos in quantum kicked top [19]. Therefore, studying the periodicity in GE is useful and interesting.

We choose the initial state to be a spin-coherent state at time $m = 0$

$$|\psi(m=0; \theta, \phi)\rangle = \psi_0 = \frac{e^{\beta J_-}}{(1 + \beta\beta^*)^j} |j, j\rangle, \quad (34)$$

parameterized by (θ, ϕ) , and chosen uniformly at random. In this $\beta = e^{i\phi} \tan(\theta/2)$, $J_- = J_x - iJ_y$, and $|j, m\rangle$ is the joint eigenstate of angular momentum operators

J^2 and J_z . The state ψ_0 is evolved using the kicked top Floquet $U(k)$ in Eq. 2 and projected onto $\{J_x, J_y, J_z\}$ at each time step. Then, purity at time m is

$$P_{su(2)}(m; \psi_0, k) = \frac{1}{j^2} \sum_{l=x,y,z} |\langle \psi_0 U^m(k) | J_l | U^m(k) \psi_0 \rangle|^2, \quad (35)$$

where $\frac{1}{j^2}$ is the normalization constant. The corresponding generalized entanglement is given by

$$GE_{su(2)}(m; \psi_0, k) = 1 - P_{su(2)}(m; \psi_0, k) \quad (36)$$

Generalized entanglement will be periodic in k (at any fixed time m) if it remains invariant under $k \rightarrow k + \kappa_j$. It can be seen that this invariance follows from the property of the kicked top operator $U(k)$ shown in Eqs. 10-13. Thus, in the case of GE, periodic nature of $U^m(k)$ leads to periodicity in GE identical to that occurring for OTOC in Eq. 15. Hence, two distinct periodicities in k are observed in GE:

$$\begin{aligned} GE_{su(2)}(m; \psi_0, k) &= GE_{su(2)}(m; \psi_0, k + 4p\pi j), \quad j \in \mathbb{Z}^+ \\ &= GE_{su(2)}(m; \psi_0, k + 2p\pi j), \quad j \in \mathbb{Z}^+ - \frac{1}{2} \end{aligned} \quad (37)$$

The period κ_j can be identified as $4p\pi j$ and $2p\pi j$ for the two cases in the above equation. This relation also holds good for generalized purity in Eq.(35) when transformed by $k \rightarrow k + \kappa_j$. The numerical simulations with kicked top dynamics shown in Fig. 5(a,b) display the expected periodicity. When $\alpha \neq n\pi/2$, where n is an integer, the periodicity of $2\pi j$ or $4\pi j$ is always satisfied, though there can exist periodicity $\kappa_j < 2\pi j$ or $\kappa_j < 4\pi j$ consistent with the general rules for $\alpha = n\pi/2$. Although we chose $su(2)$ due to its physical relevance, it is noteworthy that the periodicity in k is independent of the subspace Ω one chooses.

VI. PERIODICITY IN OBSERVATIONAL ENTROPY

Observational entropy (OE) is a unification of Gibbs and Boltzmann entropy into one. OE can be defined for both classical and quantum systems. Proposed by von Neumann [35], now there is a revived interest partly due to its relevance as a signature of chaos [16]. Consider the Hilbert space \mathcal{H} of a quantum system, partitioned into orthogonal subspaces, called macrostates $\{\mathcal{H}_i\}$, such that $\mathcal{H} = \oplus_i \mathcal{H}_i$. We denote the projection onto a macrostate \mathcal{H}_i by Π_i . Then, $\sum_i \Pi_i = \mathcal{I}_d$, since the projectors span the space. Here d is the Hilbert space dimension. Assume that these projections are the only set of measurements we can perform on the system. Then the set of projections $\chi = \{\Pi_i\}$ is called a *coarse-graining*. The dimension of a macrostate is the coarse-graining length obtained as $V_i = \text{Tr}(\Pi_i)$.

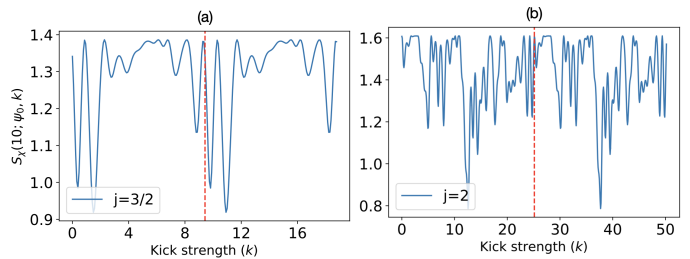


FIG. 6: Periodicity of the observational entropy with $\alpha = \pi/4$ for (a) $j = 3/2$ and $m = 10$, the red (dashed) line indicates the expected periodicity based on Eq. 37 and drawn at $\kappa_{3/2} = 2\pi j = 3\pi \approx 9.42$, (b) for $j = 2$ and $m = 10$. The red (dashed) line at $\kappa_2 = 4\pi j = 8\pi \approx 25.13$, marks one period.

Consider a state ρ in \mathcal{H} . The probability to find ρ in a macrostate \mathcal{H}_i upon projective measurements described above is $p_i = \text{Tr}(\Pi_i \rho)$. Then the observational entropy of ρ associated with the coarse-graining χ is defined as

$$S_\chi(\rho) = - \sum_i p_i \log \frac{p_i}{V_i}. \quad (38)$$

OE can be interpreted as the uncertainty associated with the system state according to an observer who performs measurements on it. The resolution of the observer determines the value OE takes. The minimum OE is the von Neumann entropy, the inherent uncertainty in the state, and the maximum OE is the maximum possible entropy allowed by the system size, $\log d$. The minimum value corresponds to the most informative measurement, where the projections are along the eigen-directions of density matrix, and the maximum value corresponds to the least informative measurement, where the measurement probabilities are uniform over the Hilbert space.

In experiments where the apparatus is unable to distinguish between two eigenstates, or if the observer can access only a part of the entire system, such coarse-graining arises naturally as a restriction. In practice, it might be easier to have coarse-grained measurements since knowing the complete density matrix would require a large number of measurements. In such cases, an observer can choose a coarse-graining given the physical problem.

From a physical perspective, coarse-graining represents a lack of complete knowledge about the system, similar to perturbation in Loschmidt echo and OTOC (OTOCs can also be seen as how an inexact time reversal due to a perturbation $W(0)$ leads to nontrivial growth of $W(t) = e^{iHt}W(0)e^{-iHt}$, leading to the spread of information and non-commutativity of $[W(t), V(0)]^2$ [11].) This ignorance manifests as a rapid increase in entropy in chaotic quantum systems, thus reflecting the underlying chaos.

OE will be periodic in k (at any fixed time m) if it remains invariant under $k \rightarrow k + \kappa_j$. To study periodicity in OE, the initial state is taken to be a random spin coherent state, defined in Eq. 34. This state is strobo-

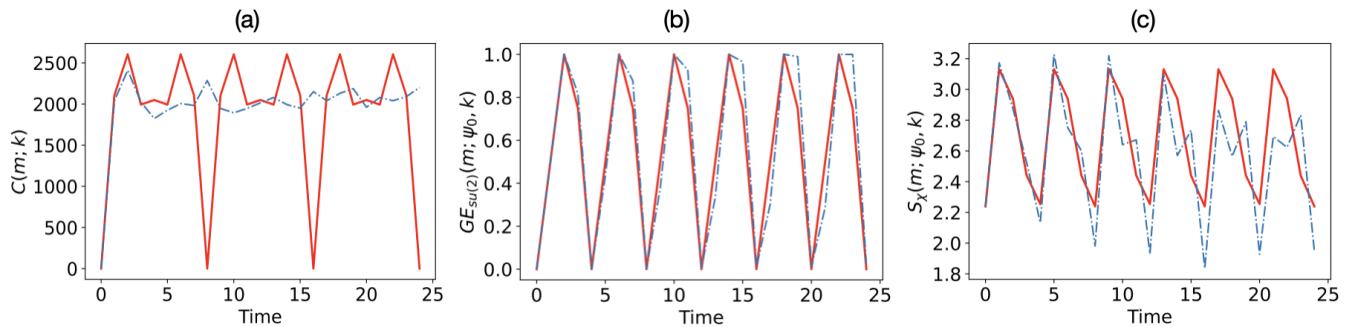


FIG. 7: (a) Periodicity of OTOC (b) generalized entanglement and (c) observational entropy for $j = 20$, at $k = N\pi/2$, where $N = 2j$ is shown in red. The blue dashed line in each figure indicates a slightly different chaoticity, $k = N\pi/2 + 0.1$. One can see that the periodicity has vanished. For GE and OE, the initial state (ψ_0) is a coherent state at $\theta = \pi/4$, $\phi = \pi/4$. Periodicity at the special k holds irrespective of the state.

scopically evolved using the kicked-top unitary $U^m(k)$ for m iterations, and a coarse-grained measurement is performed after each time step. Since we are dealing with the dynamics of OE, we rewrite the notation to illuminate its dependency on the underlying variables as follows.

$$S_\chi(m; \psi_0, k) = - \sum_i p_i^m \log \frac{p_i^m}{V_i}, \quad (39)$$

where p_i^m is the probability of observing i^{th} macrostate on measurement at time m .

For the same reasons as for generalized entanglement – periodic property of $U^m(k)$ under $k \rightarrow k + \kappa_j$ – OE also shows the same periodicity κ_j as obtained in Eq. 37. Here, we have used eigenvectors of J_z to partition the Hilbert space, with a constant coarse-graining length of two. Notably, κ_j is independent of the coarse-graining. This has been verified by partitioning the Hilbert space differently, and in each case κ_j remained unchanged. Figure 6(a,b) shows numerically simulated OE using kicked top unitary and the expected periodicity in OE are indicated by a red vertical line. It must be noted that when $\alpha = n\pi/2$, as in the case of GE, $\kappa_j < 4\pi j$ or $\kappa_j < 2\pi j$ arise while respecting the general periodicity κ_j (similar to Eq. 37).

VII. DISCUSSION AND SUMMARY

The foregoing results show that the dynamical measures display periodicity as a function of kick strength k . Existence of periodicity in these measures imply repetitions. Since periodicity κ_j depends on j , it is clear that unique behaviour of these measures – such as OTOC – are limited to $0 \leq k \leq \kappa_j$. For $k > \kappa_j$, the measures begin to repeat. Hence, it is reasonable to identify $k_{\text{max}} = 4\pi j$ for integer j , and $k_{\text{max}} = 2\pi j$ for j being half-integer. Thus, $k_{\text{max}} \propto j$. Hence, in experimental realizations of kicked top, k_{max} will provide useful guidance for the choice of

j such that repetitions of dynamical measures can be avoided.

A recent paper [36] showed that the quantum kicked top exhibits integrability at $k = N\pi/2$, where $N = 2j$, while the corresponding classical phase space is chaotic. We examined the dynamical measures of chaos at this special value of $k = k_s = N\pi/2$. It is seen that OTOC, GE and OE exhibit periodic behaviour at k_s even for $j \gg 1$. The numerical simulations shown in Fig. 7 reveals the periodicity for $j = 20$. This is different from what is anticipated based on Eq. 15. For $j \gg 1$ and the large value of kick strength, one would have expected these measures to grow and saturate in the figure. Choosing a slightly different k ruins the periodicity as seen in Fig. 7. It is noteworthy that Loschmidt echo does not show this periodicity. It is because two different chaoticity parameters, k and k' , are involved, and the overlap of their dynamics always decays, even if kick strength is chosen to be $k_s = N\pi/2$.

In summary, we have reported the periodicity properties of four different dynamical measures of chaos, namely Out-of-time ordered correlator, Loschmidt echo, generalized entanglement and observational entropy, in quantum kicked tops. Remarkably, all these measures displayed exactly the same periodicity in k : $\kappa_j = 4\pi j$ if $j \in \mathbb{Z}^+$, and $\kappa_j = 2\pi j$ if $j \in \mathbb{Z}^+ - \frac{1}{2}$. This arises from the inherent periodicity of the kicked top's unitary operator. These measures capture the properties of the underlying dynamics that is determined by the unitary operator. Since the kicking strength determines the amount of classical chaos in the system, for $k \gg 1$, the occurrence of these periodicities is an indication that the system is in the deep quantum regime.

A dynamical quantum chaos measure can be expected to manifest the scrambling in Hilbert space similar to the growth or decay of a quantum correlation function. Since the quantum dynamics of the kicked top is captured in the Floquet operator, it is imperative for the quantum measure to reflect the periodicities of the dynamics induced by the Floquet operator to be a faithful

probe into the system. Therefore, the periodicity with respect to k could act as a test to determine the reliability of a correlation function for kicked tops. This might be extended to other Floquet systems where there may be periodicities in more parameters. Also, the periodicity in k is of experimental significance since this helps in setting the parameter values in experimental platforms to avoid repeating observations. Quantum kicked tops are experimentally realized in cold-atoms, coupled superconducting qubits or NMR systems. Quantum chaos experiments require precise control over the dynamics and need

to avoid environmental decoherence. These experiments are costly, and knowing the periodicity would help one design the experiments to avoid repetitions.

VIII. ACKNOWLEDGEMENTS

MSS and SPG acknowledge funding from the QuEST program of the Department of Science and Technology (DST), Govt of India, and IISER Pune, India.

-
- [1] O. Bohigas, M.-J. Giannoni, and C. Schmit, Characterization of chaotic quantum spectra and universality of level fluctuation laws, *Physical review letters* **52**, 1 (1984).
- [2] M. V. Berry and M. Tabor, Level clustering in the regular spectrum, *Proceedings of the Royal Society of London. A. Mathematical and Physical Sciences* **356**, 375 (1977).
- [3] M. V. Berry, Regular and irregular semiclassical wavefunctions, *Journal of Physics A: Mathematical and General* **10**, 2083 (1977).
- [4] J. Wang, G. Benenti, G. Casati, and W.-g. Wang, Statistical and dynamical properties of the quantum triangle map, *Journal of Physics A: Mathematical and Theoretical* **55**, 234002 (2022).
- [5] B. Chirikov, *Les houches lecture series* 52, 443, eds. m.-j. giannoni, a. voros, and j. zinn-justin (1991).
- [6] H.-J. Stöckmann, *Quantum chaos: an introduction* (2000).
- [7] E. J. Heller and M. J. Davis, Criteria for quantum chaos, *The Journal of Physical Chemistry* **86**, 2118 (1982).
- [8] E. J. Heller, *Wavepacket dynamics and quantum chaos*, Session LII-Chaos and quantum physics (Les Houches, France, 1989) (1991).
- [9] A. I. Larkin and Y. N. Ovchinnikov, Quasiclassical method in the theory of superconductivity, *Sov Phys JETP* **28**, 1200 (1969).
- [10] S. H. Shenker and D. Stanford, Black holes and the butterfly effect, *Journal of High Energy Physics* **2014**, 1 (2014).
- [11] B. Swingle, Unscrambling the physics of out-of-time-order correlators, *Nature Physics* **14**, 988 (2018).
- [12] C. Yin and A. Lucas, Quantum operator growth bounds for kicked tops and semiclassical spin chains, *Physical Review A* **103**, 042414 (2021).
- [13] A. Peres, Stability of quantum motion in chaotic and regular systems, *Physical Review A* **30**, 1610 (1984).
- [14] R. A. Jalabert and H. M. Pastawski, Environment-independent decoherence rate in classically chaotic systems, *Physical review letters* **86**, 2490 (2001).
- [15] T. Gorin, T. Prosen, T. H. Seligman, and M. Žnidarič, Dynamics of loschmidt echoes and fidelity decay, *Physics Reports* **435**, 33 (2006).
- [16] P. Sreeram, R. Modak, and S. Aravinda, Witnessing quantum chaos using observational entropy, *Physical Review E* **107**, 064204 (2023).
- [17] F. Buscemi, J. Schindler, and D. Šafránek, Observational entropy, coarse-grained states, and the petz recovery map: information-theoretic properties and bounds, *New Journal of Physics* **25**, 053002 (2023).
- [18] L. Viola and W. G. Brown, Generalized entanglement as a framework for complex quantum systems: purity versus delocalization measures, *Journal of Physics A: Mathematical and Theoretical* **40**, 8109 (2007).
- [19] Y. S. Weinstein and L. Viola, Generalized entanglement as a natural framework for exploring quantum chaos, *Europhysics Letters* **76**, 746 (2006).
- [20] V. Latora and M. Baranger, Kolmogorov-sinai entropy rate versus physical entropy, *Physical Review Letters* **82**, 520 (1999).
- [21] F. Haake, M. Kuś, and R. Scharf, Classical and quantum chaos for a kicked top, *Zeitschrift für Physik B Condensed Matter* **65**, 381 (1987).
- [22] F. Haake, *Quantum Signatures of Chaos* (Springer-Verlag, Berlin, Heidelberg, 2006).
- [23] S. Chaudhury, A. Smith, B. Anderson, S. Ghose, and P. S. Jessen, Quantum signatures of chaos in a kicked top, *Nature* **461**, 768 (2009).
- [24] C. Neill, P. Roushan, M. Fang, Y. Chen, M. Kolodrubetz, Z. Chen, A. Megrant, R. Barends, B. Campbell, B. Chiaro, *et al.*, Ergodic dynamics and thermalization in an isolated quantum system, *Nature Physics* **12**, 1037 (2016).
- [25] V. Krithika, V. Anjusha, U. T. Bhosale, and T. Mahesh, Nmr studies of quantum chaos in a two-qubit kicked top, *Physical Review E* **99**, 032219 (2019).
- [26] S. Dogra, V. Madhok, and A. Lakshminarayan, Quantum signatures of chaos, thermalization, and tunneling in the exactly solvable few-body kicked top, *Physical Review E* **99**, 062217 (2019).
- [27] P. Sreeram, V. Madhok, and A. Lakshminarayan, Out-of-time-ordered correlators and the loschmidt echo in the quantum kicked top: how low can we go?, *Journal of Physics D: Applied Physics* **54**, 274004 (2021).
- [28] U. T. Bhosale and M. Santhanam, Periodicity of quantum correlations in the quantum kicked top, *Physical Review E* **98**, 052228 (2018).
- [29] B. Yan, L. Cincio, and W. H. Zurek, Information scrambling and loschmidt echo, *Physical review letters* **124**, 160603 (2020).
- [30] P. Zanardi and D. A. Lidar, Purity and state fidelity of quantum channels, *Physical Review A* **70**, 012315 (2004).
- [31] I. García-Mata, A. J. Roncaglia, and D. A. Wisniacki, Lyapunov decay in quantum irreversibility, *Philosophical Transactions of the Royal Society A: Mathematical, Physical and Engineering Sciences* **374**, 20150157 (2016).

- [32] H. Barnum, E. Knill, G. Ortiz, R. Somma, and L. Viola, A subsystem-independent generalization of entanglement, *Physical Review Letters* **92**, 107902 (2004).
- [33] Q. Chaos, by ha cerdeira, r. ramaswamy, mc gutzwiller and g. casati (1991).
- [34] A. Peres, *Quantum theory: concepts and methods*, Vol. 72 (Springer, 1997).
- [35] J. von Neumann, Proof of the ergodic theorem and the h-theorem in quantum mechanics: Translation of: Beweis des ergodensatzes und des h-theorems in der neuen mechanik, *The European Physical Journal H* **35**, 201 (2010).
- [36] H. Sharma and U. T. Bhosale, Violation of bohigas-giannoni-schmit conjecture using an integrable many-body floquet system, arXiv preprint arXiv:2307.14122 (2023).

SUPPLEMENTARY

The time evolution unitary obtained from the kicked top Hamiltonian is given by

$$U = \exp\left(-i\frac{k}{2j}J_z^2\right)\exp(-i\alpha J_y). \quad (40)$$

This unitary causes precession of the state about the Y -axis by an angle α followed by an impulsive rotation about the Z -axis. Alternatively, in the Heisenberg picture, the evolution of the angular momentum operator can be obtained as follows:

$$J'_i = U^\dagger J_i U. \quad (41)$$

The recursion relations for the angular momentum components are obtained as follows.

$$\begin{aligned} J'_x &= \frac{1}{2}(J_x \cos \alpha + J_z \sin \alpha + iJ_y)e^{i\frac{k}{j}(J_z \cos \alpha - J_x \sin \alpha + \frac{1}{2})} \\ &\quad + \text{h.c.} \\ J'_y &= \frac{1}{2i}(J_x \cos \alpha + J_z \sin \alpha + iJ_y)e^{i\frac{k}{j}(J_z \cos \alpha - J_x \sin \alpha + \frac{1}{2})} \\ &\quad + \text{h.c.} \\ J'_z &= -J_x \sin \alpha + J_z \cos \alpha. \end{aligned} \quad (42)$$

The classical limit can be obtained by taking $j \rightarrow \infty$. Defining $X = \left\langle \frac{J_x}{j} \right\rangle$, $Y = \left\langle \frac{J_y}{j} \right\rangle$, and $Z = \left\langle \frac{J_z}{j} \right\rangle$, where the expectation values are with respect to spin-coherent

states, we get the classical map:

$$\begin{aligned} X' &= (X \cos \alpha + Z \sin \alpha) \cos[k(Z \cos \alpha - X \sin \alpha)] \\ &\quad - Y \sin[k(Z \cos \alpha - X \sin \alpha)], \\ Y' &= (X \cos \alpha + Z \sin \alpha) \sin[k(Z \cos \alpha - X \sin \alpha)] \\ &\quad + Y \cos[k(Z \cos \alpha - X \sin \alpha)], \\ Z' &= -X \sin \alpha + Z \cos \alpha. \end{aligned} \quad (43)$$

Taking $\alpha = \pi/2$, the above map simplifies, and takes the form [21]

$$\begin{aligned} X' &= Z \cos(kX) + Y \sin(kX), \\ Y' &= -Z \sin(kX) + Y \cos(kX), \\ Z' &= -X. \end{aligned} \quad (44)$$

The classical map for the case of $\alpha = \pi/2$, at four different values of k are shown in Fig. 8. The phase space is mostly regular at $k = 0.5$. As k increases, the regular structures disappear and the phase space becomes increasingly chaotic for $k \gg 1$. As seen in Fig. 8(d), the dynamics is predominantly chaotic.

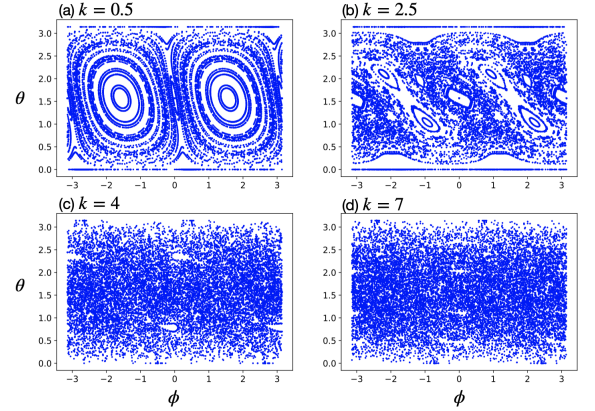


FIG. 8: Classical phase space for $\alpha = \pi/2$ at four different chaoticity values, a) $k = 0.5$, b) $k = 2.5$, c) $k = 4$ and d) $k = 7$.